Effects of annealing rate and morphology of sol–gel derived ZnO on the performance of inverted polymer solar cells*

Yu Xuan(余 璇), Hu Zi-Yang(胡子阳), Huang Zhen-Hua(黄振华), Yu Xiao-Ming(于晓明), Zhang Jian-Jun(张建军)†, Zhao Geng-Shen(赵庚申), and Zhao Ying(赵 颖)

Institute of Photo-electronic Thin Film Devices and Technology of Nankai University, Key Laboratory of Photo-electronic Thin Film Devices and Technology of Tianjin, Key Laboratory of Opto-electronic Information Science and Technology for Ministry of Education, Tianjin 300071, *China*

(Received 25 March 2013; revised manuscript received 22 April 2013)

The effects of annealing rate and morphology of sol–gel derived zinc oxide (ZnO) thin films on the performance of inverted polymer solar cells (IPSCs) are investigated. ZnO films with different morphologies are prepared at different annealing rates and used as the electron transport layers in IPSCs. The undulating morphologies of ZnO films fabricated at annealing rates of 10 °C/min and 3 °C/min each possess a rougher surface than that of the ZnO film fabricated at a fast annealing rate of 50 °C/min. The ZnO films are characterized by atomic force microscopy (AFM), optical transmittance measurements, and simulation. The results indicate that the ZnO film formed at 3 °C /min possesses a good-quality contact area with the active layer. Combined with a moderate light-scattering, the resulting device shows a 16% improvement in power conversion efficiency compared with that of the rapidly annealed ZnO film device.

Keywords: polymer solar cells, zinc oxide thin film, morphology, annealing

PACS: 88.40.jr, 77.55.hf, 81.40.Ef **DOI:** 10.1088/1674-1056/22/11/118801

1. Introduction

In recent years, much attention has been paid to the polymer bulk-heterojunction (BHJ) solar cells (PSCs) due to their low manufacturing cost and potential application in flexible and large-area solar cells.[1–7] The inverted polymer solar cells (IPSCs) exhibit competitive performances and offer better stabilities compared with the traditional BHJ solar cells.[8–12] In an IPSC, a thin film of N-type metal oxide, such as titanium oxide (TiO_x),[13] cesium carbonate (Cs_2CO_3),[14] or ZnO,[15–17] is used as a cathode buffer layer to lower the work function of the indium tin oxide (ITO) substrate. ZnO is an attractive material due to its non-toxicity, low cost, excellent stability, high electron mobility, and high transparency in the visible wavelength range.[18] There are many techniques that can be used to prepare ZnO films;[19–22] the sol–gel process is believed to hold the greatest potential for large-scale commercial fabrication due to no need of a vacuum process. Various nano-structures of ZnO films have been prepared by solution processing to enable efficient charge transport,[18,23] indicating that the ZnO film morphology plays a very important role in determining the performance of IPSCs.[20,24] The temperature at which ZnO is annealed is a significant factor in determining the morphology,[21,25,26] structural and optical properties[27] of the thin films. However, the effects of the annealing rate and the morphology of the ZnO thin film on the performance of IPSC are still not clear. In order to investigate the relevance between ZnO annealing rate and morphology and the resulting influence on the device performance, we study IPSCs using ZnO thin films prepared from a zinc acetate dihydrate solution as the electron transport layers (ETLs). It is shown that the morphology of the ZnO thin film can be controlled by adjusting the heating process, and the device performance can be effectively improved correspondingly. The effects of the ZnO film morphology on the characteristics of IPSC are discussed in detail.

2. Experiments

2.1. Materials and device manufacture

In this study, the ZnO sol–gel solution consisted of zinc acetate dihydrate ($Zn(CH_3COO)_2{\cdot}2H_2O$) and ethanolamine ($C_2H_7NO$) in ethanol ($C_2H_5OH$),[25] the solution became homogeneous and transparent after stirring at 60 °C for 3 h. Having aged at room temperature for 24 h, the ZnO sol–gel solution was spin-coated on cleaned ITO-glass substrates at a speed of 2000 rpm for 40 s. The samples were then annealed on a hot plate from room temperature (22 °C) to 270 °C at three different rates (50 °C/min, 10 °C/min, 3 °C/min). An active layer was spin-coated onto the ZnO layer using a solution consisting of a poly (3-hexylthiophene) (P3HT): [6, 6]-phenyl C_{61} butyric acid methyl ester (PCBM) blend with a weight ratio of 1:0.8 in chlorobenzene. A combination of spin-coating rates, 250 rpm (3 s) and 1000 rpm (10 s), was used. The thickness of the active layer was ∼ 180 nm. The substrates were placed in covered Petri dishes and solvent annealed for 2 h.

*Project supported by the National Basic Research Program of China (Grant Nos. 2011CBA00705, 2011CBA00706, and 2011CBA00707) and the National Natural Science Foundation of China (Grant No. 61377031).

†Corresponding author. E-mail: jjzhang@nankai.edu.cn

© 2013 Chinese Physical Society and IOP Publishing Ltd

MoO_3 (∼ 3 nm) and Ag (∼ 70 nm) were thermally evaporated successively on the active layer under a pressure 10^{-4} Pa and then thermally annealed at 120 °C for 10 min in an oven under atmospheric pressure. The active area of the devices was 0.08 cm^2 determined by the shade mask. The structure of the IPSC is shown in Fig. 1.

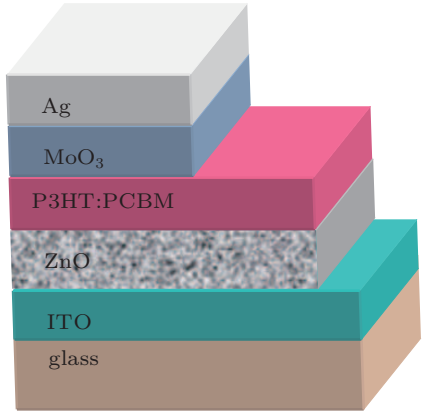


Fig. 1. (color online) Schematic diagram of inverted polymer solar cell with ZnO film.

2.2. Measurement

The surface of the ZnO thin film was observed by optical microscopy (Nikon ECLIPSE Ti-u). The surface morphology of the thin film was characterized by atomic force microscopy (AFM) (Seiko SPA-400 SPM UNIT). The transmittance spectra of the ZnO-coated substrates were measured by a Cary spectrophotometer (Cary 5000UV–VIS). The current density–voltage (J–V) characteristics of the film was measured with a Keithley 4200 sourcemeter under the illumination of an AM 1.5 G (100 mW/cm^2) solar simulator.

3. Results and discussion

3.1. Surface morphology

The only difference among all of the IPSCs investigated in this study was the annealing process of the ZnO thin films; all other parameters were kept constant. Optical microscopy was used to evaluate the surface quality of the ZnO thin film. Some fissures and small holes were observed on the surfaces of the ZnO films heated at 50 °C/min (Fig. 2(a)) and 10 °C/min (Fig. 2(b)), respectively. With a high heating rate, the stress force could not be released during the crystallization of the ZnO thin film. In addition, as is well known, the ZnO crystal growth is disturbed by the solvent when the solvent is not vaporized entirely. If the heating rate is slow enough, there is sufficient time for the solvent to evaporate and the structure to relax before crystallization to form a denser film.[25] The 3 °C/min film presents a more homogeneous (see Fig. 2(c)) coverage on the ITO substrate compared with the other films, preventing the formation of a current leakage pathway, which typically arises from the direct contact between an uncovered ITO substrate and the active layer.

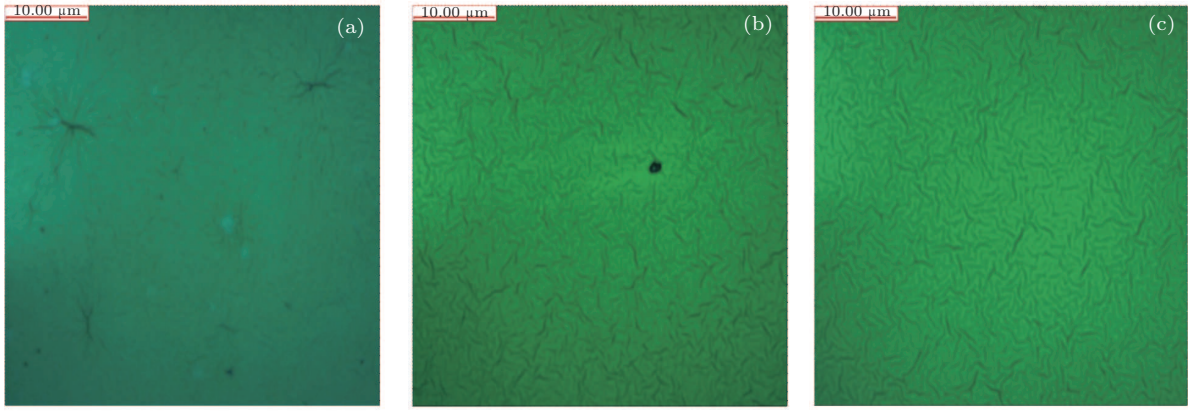


Fig. 2. (color online) Optical microscopy images of ZnO films deposited on ITO substrates at heating rates of (a) 50 °C/min, (b) 10 °C/min, and (c) 3 °C/min. The scale bar represents 10 μm.

The AFM images of the ZnO films are shown in Fig. 3. The 50 °C/min film shows ZnO nanoparticles with a surface root-mean-square roughness (RMS) of 8 nm, which becomes smoother after coating with the active layer (Fig. 3(g)). The 10 °C/min film shows a much coarser texture with sharp hill-like features with mean height of ∼70 nm and width of ∼ 200 nm; the distance from one ridge to its adjacent ridge is ∼ 600 nm. Ridges on the rough surface of the film can still be observed (Fig. 3(b)) even though it is covered with an active layer (Fig. 3(h)). The surface roughness of ZnO has a direct influence on the active layer, and it can transfer the roughness from the anode to the interface between the ZnO thin film and the active layer.[19] The 3 °C/min film shows ridges with height of ∼ 45 nm and width of ∼ 450 nm and appears as a great pile of thick ropes, between which the distance is very small. We find that the ridge on the surface of the ZnO thin film annealed at a slow rate is lower in height and wider in width.

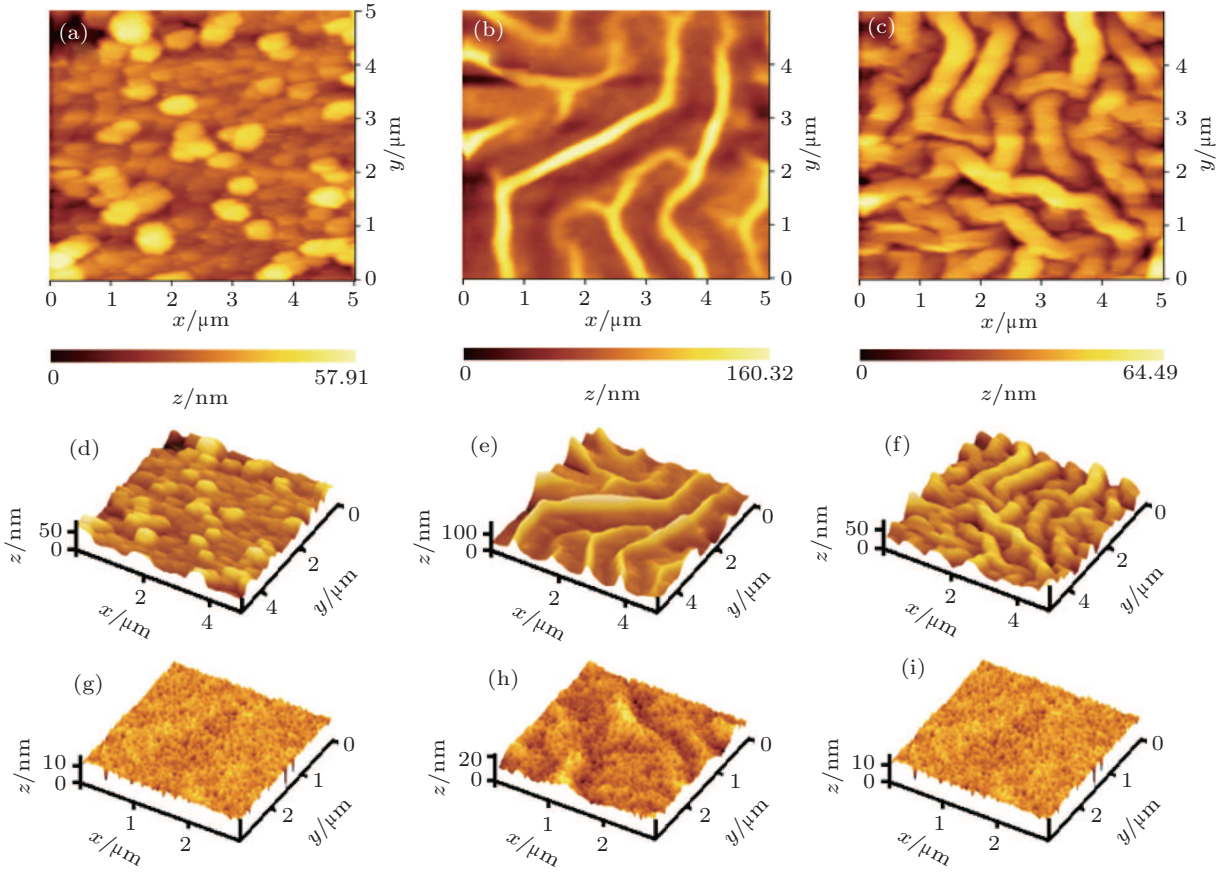


Fig. 3. (color online) (a)–(c) AFM images of the flat surfaces and (d)–(f) the corresponding stereoscopic views of ZnO thin films annealed at rates of 50 °C/min, 10 °C/min, and 3 °C/min from room temperature to 270 °C, respectively. The films in panels (g)–(i) each are covered with a P3HT: PCBM layer.

3.2. Optical properties

The transmittance of the ZnO film is very important for the performance of IPSC. We measured the total and spectral transmittances of the ZnO films. The three ZnO thin films show good optical transmittances of over 80% at wavelengths ranging from 400 nm to 1000 nm (Fig. 4(a)). We also calculated the haze $((T_{\text{total}} - T_{\text{spectral}})/T_{\text{total}})$ of all the ZnO layers, which qualitatively describe the light-scattering properties of textured films.[28] The results are displayed in the inset of Fig. 4(a), suggesting that film B presents better light-scattering properties under the same conditions.

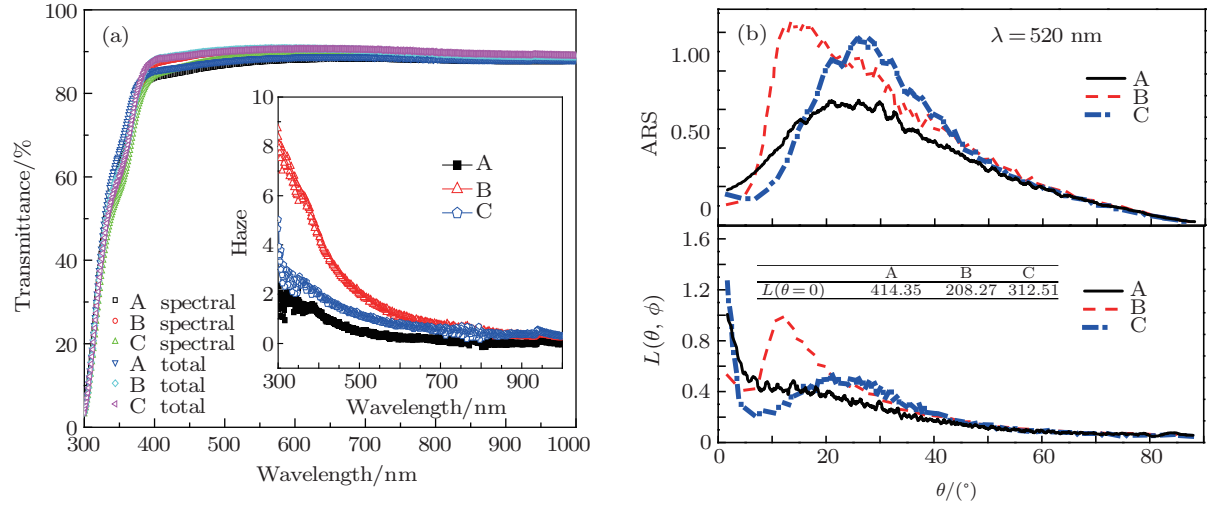


Fig. 4. (color online) (a) Transmittance spectra and variations in haze (inset) for the ZnO thin films, (b) calculated ARS and L results for ZnO thin films at 520 nm.

To further study the scattering properties of the three ZnO films, the phase model reported in Refs. [29] and [30] was used to calculate the angular dependence of the scattered light. The calculated radiance L and angular resolved scattering (ARS) of the textured interfaces are shown in Fig. 4(b). It is apparent that the range and amplitude of radiance $L(\theta > 0)$ increase as the morphology becomes more textured, and simultaneously, the $L(\theta = 0)$ drops sharply (see the inserted table in Fig. 4(b)). These results indicate that the amount of light scattered at different angles increases as the morphology changes in the order of A, C, B. Film B is determined to have the largest amplitudes over the entire range of radiance, which is consistent with the haze results.

3.3. Application in IPSCs

The current–voltage (J–V) characteristics of the IPSCs based on the ZnO thin films fabricated in this study are shown in Fig. 5(a). The external quantum efficiencies (EQEs) of the cells are shown in Fig. 5(b), and the device performances are summarized in Table 1. Device C, whose ZnO thin film is annealed at 3 °C/min, clearly shows better performance than the other devices. It displays a short-circuit current (J_{sc}) of 8.32 mA/cm^2, an open-circuit voltage (V_{oc}) of 0.55 V, and a filling factor (FF) of 52.3% for an overall power conversion efficiency (PCE) of 2.42%. Meanwhile, the devices featuring films A and B processed at faster annealing rates show the efficiencies of 2.09% and 2.03%, respectively.

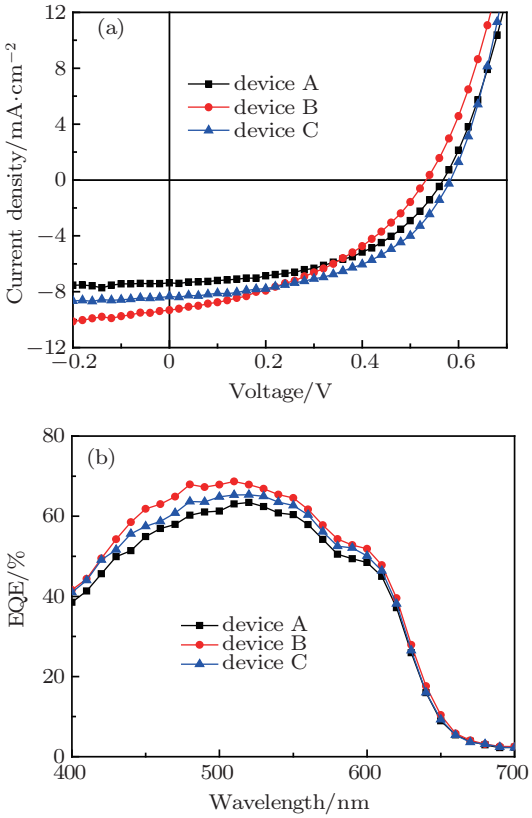


Fig. 5. (color online) (a) Current density–voltage (J–V) characteristics under the illumination of AM 1.5 G (100 mW/cm^2) solar simulator, (b) the EQE curves for devices A, B, and C.

Table 1. Detailed performance parameters of the IPSCs.

Device	RMS of ZnO/nm	RMS of ZnO with active layer/nm	J_{sc}/mA·cm^{-2}	V_{oc}/V	FF/%	PCE/%	R_{sh}/Ω·cm^2	R_s/Ω·cm^2
A	8	1.2	7.36	0.55	51.7	2.09	528.9	22.5
B	27	2.7	9.31	0.52	41.7	2.03	207.3	20.5
C	10	1.4	8.32	0.55	52.3	2.42	546.4	18.1
No ZnO	–	–	4.08	0.37	41.1	0.62	300.4	35.4

The excellent performance of device C could be attributed to two factors. First, the slow annealing process results in the good continuity of the film and good coverage over the ITO substrate. The continuity of film is beneficial to extracting charge and blocking hole transport, thus improving the shunt resistance (R_{sh}) and FF.[23] Second, film C has a relatively homogeneous and gentle morphology, which improves the wetting of the active layer due to the closer contact to the P3HT:PCBM layer. At the same time, the moderate RMS roughness increases the contact area between the substrate and the active layer, leading to the swift extraction of carriers; moreover, the moderate scattering of the device contributes to an increase in light absorption without deteriorating the FF and V_{oc}, resulting in a high PCE.

The film heated at 10 °C/min has a large surface contact area at the ZnO/ P3HT:PCBM interface and the best light-scattering ability; thus, device B possesses a J_{sc} of 9.31 mA/cm^2. This enhancement is also reflected in the increased quantum efficiency of device B (see Fig. 5(b)). However, film B shows small holes as previously mentioned. The contact quality between the ZnO film and the active layer is reflected in shunt resistance R_{sh} and series resistance R_s of IPSCs.[24] Due to the degradation of the shunt resistance (207.3 Ω·cm^2) and the recombination of charge carriers, the PCE of device B is reduced to 2.03%, i.e., the V_{oc} and FF are adversely affected.

Device A presents the lowest J_{sc} among the three devices (7.36 mA/cm^2). This is attributed to the fast heating rate of 50 °C/min, which leads to the formation of surface fissures, thereby forming a current leakage pathway, in addition to the

minimal light-scattering ability of the device. We also prepared a device without the ZnO layer to investigate its role in electron transport. Because the Fermi level of ZnO (4.3 eV) matches the lowest unoccupied molecular orbital (LUMO) of the acceptor PCBM (4.3 eV), the electron transfer is more convenient and effective.[20] As shown in Table 1, compared with the device without a ZnO ETL, the improved device performances could be attributed to the excellent ability of the ZnO film to transport and extract electrons.

4. Conclusion

We evaluated the performances of IPSCs featuring sol–gel derived ZnO films as ETLs. Three ZnO films with different morphologies and thus different scattering properties were formed by adjusting the rate of annealing. The ZnO film annealed at a rate of 10 °C/min, with the best light-scattering ability, can enhance the resulting device J_{sc}, though the morphology needs to be improved to reduce the recombination and achieve a high efficiency. The ZnO film formed at 3 °C/min, exhibits good contact quality with the active layer in combination with a moderate light-scattering ability enhanced device PCE. Our research provides a simple way of optimizing the surface topography of ZnO thin films to obtain high-performance IPSCs.

References

[1] Yu G, Gao J, Hummelen J C, Wudl F and Heeger A J 1995 *Science* **270** 1789

[2] Li Y F 2012 *Acc. Chem. Res.* **45** 723

[3] Krebs F C, Nielsen T D, Fyenbo J, Wadstrøm M and Pedersen M S 2010 *Energy Environ. Sci.* **3** 512

[4] Yu H Z and Peng J B 2008 *Chin. Phys. B* **17** 3143

[5] Huo L J, Zhang S Q, Guo X, Xu F, Li Y F and Hou J H 2011 *Angew. Chem.* **123** 9871

[6] Yang S P, Li N, Li G, Shi J B, Li X W and Fu G S 2013 *Acta Phys. Sin.* **62** 014702 (in Chinese)

[7] Yu H Z and Wen Y X 2011 *Acta Phys. Sin.* **60** 038401 (in Chinese)

[8] Yang T, Wang M, Duan C, Hu X, Huang L, Peng J, Huang F and Gong X 2012 *Energy Environ. Sci.* **5** 8208

[9] Wu J, Guo X Y and Xie Z Y 2012 *Chin. Phys. Lett.* **29** 098801

[10] Tan Z A, Zhang W Q, Zhang Z G, Qian D P, Huang Y, Hou J H and Li Y F 2012 *Adv. Mater.* **24** 1476

[11] Krebs F C and Norman K 2007 *Prog. Photovoltaics.* **15** 697

[12] Jørgensen M, Norrman K and Krebs F C 2008 *Sol. Energy Mater. Sol. Cells* **92** 686

[13] Weickert J, Sun H, Palumbiny C, Hesse H C and Mende L S 2010 *Sol. Energy Mater. Sol. Cells* **94** 2371

[14] Liao H H, Chen L M, Xu Z, Li G and Yang Y 2008 *Appl. Phys. Lett.* **92** 173303

[15] Chu T Y, Tsang S W, Zhou J, Verly P G, Lu J, Beaupre S, Leclerc M and Tao Y 2012 *Sol. Energy Mater. Sol. Cells* **96** 155

[16] Chang C Y, Wu C E, Chen S Y, Cui C, Cheng Y J, Hsu C S, Wang Y L and Li Y F 2011 *Angew. Chem. Int. Ed.* **50** 9386

[17] Stubhan T, Oh H, Pinna L, Krantz J, Litzov I and Brabec C J 2011 *Org. Electron.* **12** 1539

[18] Hu Z Y, Zhang J J, LiuY, Hao Z H, Zhang X D and Zhao Y 2011 *Sol. Energy Mater. Sol. Cells* **95** 2126

[19] Lare Y, Godoy A, Cattin L, Jondo K, Abachi T, Diaz F R, Morsli M, Napo K, del Valle M A and Berne J C 2009 *Appl. Surf. Sci.* **255** 6615

[20] Huang J, Yin Z and Zheng Q 2011 *Energy Environ. Sci.* **4** 3861

[21] Nga Z N, Chana K Y and Tohsophon T 2012 *Appl. Surf. Sci.* **258** 9604

[22] Lu Z L, Zou W Q, Xu M X and Zhang F M 2010 *Chin. Phys. B* **19** 076101

[23] Sekine N, Chou C H, Kwan W L and Yang Y 2009 *Org. Electron.* **10** 1473

[24] Liang Z, Zhang Q, Wiranwetchayan O, Xi J, Yang Z, Park K, Li C and Cao G 2012 *Adv. Funct. Mater.* **22** 2194

[25] Ohyama M, Kozuka H and Yoko T 1997 *Thin Solid Films* **306** 78

[26] Saleem M, Fang L, Huang Q L, Li DC, Wu F, Ruan H B and Kong C Y 2012 *Surf. Rev. Lett.* **19** 1250055

[27] Jijoy P M, George V and Jacob M 2012 *Chin. Phys. B* **21** 078104

[28] Hu Z Y, Zhang J J and Zhao Y 2012 *J. Appl. Phys.* **111** 104516

[29] Domine D, Haug F J, Battaglia C and Ballif C 2010 *J. Appl. Phys.* **107** 044504

[30] Battaglia C, Boccard M, Haug F J and Ballif C 2012 *J. Appl. Phys.* **112** 094504